

Raman efficiency in SiGe alloys

A. Picco, E. Bonera, E. Grilli, and M. Guzzi

Dipartimento di Scienza dei Materiali, Università degli Studi di Milano-Bicocca, via Cozzi 53, I-20125 Milano, Italy

M. Giarola and G. Mariotto

Dipartimento di Informatica, Università di Verona, strada le Grazie 15, I-37134 Verona, Italy

D. Chrastina and G. Isella

LNESS, Dipartimento di Fisica, Politecnico di Milano, Polo Regionale di Como, via Anzani 42, I-22100 Como, Italy

(Received 8 June 2010; revised manuscript received 26 July 2010; published 21 September 2010)

Raman spectroscopy is commonly used for the optical characterization of structural properties of SiGe alloys but a measurement of the Raman efficiency as a function of excitation wavelength and concentration is still lacking. This information is nevertheless important for the interpretation of data, especially for the analysis of inhomogeneous samples. In this work, the relative Raman efficiency of $\text{Si}_{1-x}\text{Ge}_x$ alloys has been obtained for several excitation energies as a function of the composition x with steps of $\Delta x \sim 0.02$ across the whole composition range. We observed resonances in correspondence of the $E_1/E_1 + \Delta_1$ and $E_0/E_0 + \Delta_0$ transitions. For a fixed excitation energy the efficiency varies of about 2 orders of magnitude vs the composition of the alloy, while, for a fixed composition, we observed a change in efficiency of up to 3 orders of magnitude depending on the excitation energy. The maximum scattering efficiency at resonance decreases by an order of magnitude when moving from silicon-rich to germanium-rich alloys. The data are discussed in terms of the polarizability and compared to the literature relative to pure silicon and germanium. The data reported in this paper can be used to design experiments under resonant conditions to selectively probe different regions in inhomogeneous samples.

DOI: [10.1103/PhysRevB.82.115317](https://doi.org/10.1103/PhysRevB.82.115317)

PACS number(s): 78.20.-e, 78.30.Er

I. INTRODUCTION

Raman spectroscopy allows the composition and strain state of $\text{Si}_{1-x}\text{Ge}_x$ alloys to be measured. In the past, several works were dedicated to the interpretation of the spectra and the extraction of structural information but most of them did not take into account the Raman efficiency S , defined as the probability for a photon to be scattered in the unit path length within the solid. In fact, the efficiency can vary significantly with the excitation energy and the composition x of the alloy. However, a comprehensive measurement of the Raman efficiency as a function of the excitation wavelength for the full range of compositions is still missing in the literature.

The enhancement in the Raman efficiency for energies in the neighborhood of direct transitions in semiconductors has been studied both experimentally and theoretically.¹⁻⁴ For the case of Si-Ge alloys, besides the works about pure silicon⁴ and germanium,² there are only a few data in the literature only for values of the Ge fraction x close to 0.7.^{1,5} In other works, the efficiency has been measured as a function of the excitation energy to obtain information about the electronic properties of strained or confined systems.⁶⁻¹⁰ On the other hand, the variation in the Raman efficiency in SiGe as a function of the composition for a given excitation energy has not been explored in detail. This information has nevertheless a high practical interest for the interpretation of spectra, especially from inhomogeneous samples, such as multilayers or self-assembled nanostructures.^{5,11} Similarly, the knowledge of S as a function of x opens the possibility of designing dedicated experiments for the selective probing of different regions of inhomogeneous materials.¹² In this work, we present a systematic and comprehensive measurement of

the Raman efficiency in SiGe for several excitation energies and for the whole composition range.

II. EXPERIMENT

The experiment is based on the measure of the Raman efficiency in a thick graded layer with a smooth variation in x from pure silicon to pure germanium, grown by low-energy plasma-enhanced chemical vapor deposition.¹³ This graded layer is expected to be relaxed since its thickness largely exceeds the critical value beyond which plastic relaxation is known to occur. In order to span the entire range of compositions, the sample was a graded layer on top of a (001) c -Si substrate with composition varying linearly from $x=0$ to $x=1$ with a composition variation equal to $\Delta x=0.05$ for each micrometer. The graded layer was capped by a $1\text{-}\mu\text{m}$ -thick film of pure germanium (see the inset of Fig. 1). The sample was cleaved along a (110) plane and observed in crossview. In the remainder of the paper we will use the following reference system: $\mathbf{z}' \parallel [001]$ is the growth direction, $\mathbf{x}' \parallel [1\bar{1}0]$ is the intersection of the growth plane and the cleaved surface, and $\mathbf{y}' \parallel [110]$ is the normal to the cleaved surface. For each excitation energy, we collected a set of spectra in back-scattering geometry along \mathbf{y}' , scanning the focus of the microscope along \mathbf{z}' with steps of $0.3 \mu\text{m}$, corresponding to a variation of $\Delta x=0.016$ in composition. According to Porto's notation,¹⁴ the experimental geometry for these measurements was $\mathbf{y}'(\mathbf{x}', \mathbf{x}')-\mathbf{y}'$.

The Raman measurements were carried out in air at room temperature, under excitation at several wavelengths, i.e., laser lines at 1.96, 2.33, 2.54, 2.71, 3.08, and 3.40 eV, in nearly

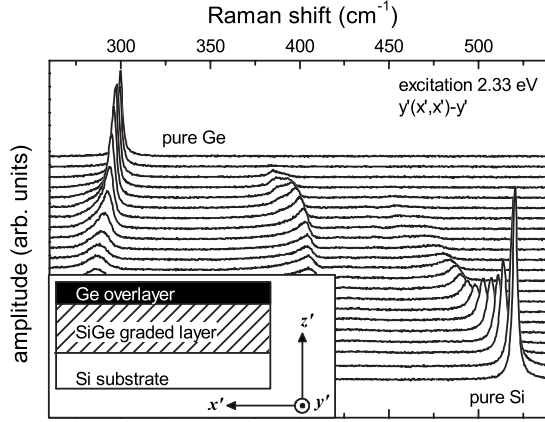


FIG. 1. Selected spectra from a linescan along z' spanning from pure Si to pure Ge. The three main bands of the alloy are visible at about 300, 400, and 500 cm^{-1} . This linescan was obtained with a 2.33 eV excitation. The inset shows the sketch of the sample cross view of the sample with the reference system adopted for the measurement.

backscattering geometry. The scattered radiation was dispersed with a Jasco (model R800) double 800 mm spectrometer when notch filters were available, or with an Horiba-Jobin Yvon (model T64000) triple 640 mm spectrometer in the other cases, using the double premonochromator to filter the elastically scattered radiation. The Stokes component of Raman scattering was detected at the exit window of the spectrometers with a cooled charge coupled device (256×1024 pixels). The spectrometers were coupled to microscopes equipped with a piezoelectric positioning stage having a nanometer scale precision. The spatial resolution achievable was less than 1 μm . The laser power was always appropriately limited in order to prevent the sample from heating.

In order to check the consistency of the whole procedure, in addition to the graded layer, we measured the Raman spectra of a set of individual layers having a compositional parameter $x=0.00, 0.20, 0.40, 0.60, 0.80, 1.00$, respectively. These samples, described in Ref. 15, were 1 μm thick, deposited on a thick graded buffer layer, and characterized by both Raman and x-ray diffraction. For these samples the experimental geometry was $z'(x', -)z'$, where the dash signifies that no polarization analysis of the scattered radiation was performed.

III. RESULTS AND DISCUSSION

A typical SiGe first-order Raman spectrum shows three bands attributed to Ge-Ge, Si-Ge, and Si-Si modes¹⁶ with peak wavenumbers of about 300 cm^{-1} , 400 cm^{-1} , and 500 cm^{-1} , respectively. Figure 1 reports some of the spectra collected along the scanning direction z' under excitation at 2.33 eV: the sequence of spectra shows the transition from Si to Ge. Spectra recorded through repeated scans in different regions of the sample revealed that the intensity of the bands was reproducible within 5%. For each spectrum, the energy position of the bands maxima allowed to measure the local

strain and the alloy composition. Using the calibrations derived in Ref. 15 the composition and the in-(001)plane biaxial strain were checked; the strain was found to be in the range between 0.0% and 0.3%, probably due to the mismatch of thermal expansion coefficients.¹⁷

A. Determination of Raman efficiency

Starting from the intensity of the Raman spectra, we want now to extract the efficiency. We recall that the Raman efficiency S , having the dimensions of an inverse length, is defined as¹⁸

$$S = \frac{\omega_s^4 \hbar (n+1)}{32 \pi^2 c^4 \omega_b} \left| \mathbf{e}_s \cdot \frac{\partial \chi}{\partial \xi} \cdot \mathbf{e}_i \right|^2. \quad (1)$$

In this equation the Raman tensor $\partial \chi / \partial \xi$, defined as the derivative of the dielectric susceptibility χ with respect to the phonon normal coordinate ξ , is responsible for the resonance phenomena; \mathbf{e}_i and \mathbf{e}_s are the unit vectors giving the polarization of the incident and scattered photons; ω_b is the phonon frequency; ω_s is the scattered photon frequency; n is the Bose-Einstein distribution function; and c is the speed of light in vacuum.

We measured the relative values of S with respect to a standard reference sample of (110) CaF_2 , observed under the same experimental conditions and geometry, as in Ref. 4. In order to extract the values of S from the spectra of Fig. 1, we considered I_{SiGe} , the sum of the integrated intensity of the three SiGe bands, and the integrated intensity I_{CaF_2} . Assuming a small solid angle Ω of collection, the values of S and I are linked by the relationship

$$\frac{I_{\text{SiGe}}}{I_{\text{CaF}_2}} = \frac{S_{\text{SiGe}}^* \Omega_{\text{SiGe}}}{S_{\text{CaF}_2}^* \Omega_{\text{CaF}_2}} \quad (2)$$

where the symbol S^* is the following function of S :

$$S^* = S \frac{1 - \exp[-(S + \alpha_i + \alpha_s)L]}{S + \alpha_i + \alpha_s} (1 - R_i)(1 - R_s). \quad (3)$$

The dimensionless quantity S^* represents the effective scattering efficiency¹⁸ and takes into account that I also depends on a number of parameters which are not directly related to the Raman efficiency of the alloy. These parameters are the absorption coefficient α , the reflection coefficient R of the sample surface, and the probed depth L beneath the sample surface. The values of α and R were interpolated from data in the literature.^{19,20} Again, the indexes i and s of both α and R functions refer to the incident and scattered radiation, respectively.

The results of the efficiency determination are shown in Fig. 2, where the ratio between the values of S for SiGe and CaF_2 is shown as a function of the alloy composition for each value of the excitation energy. The data in this Figure are affected by uncertainties both from the experimental procedure and the evaluation of the optical functions extracted from literature. In all plots we estimate an overall uncertainty of less than 20% on the maximum amplitude of the bands, caused mainly by the interpolation of the optical functions found in the literature. The confirmation of the consistency

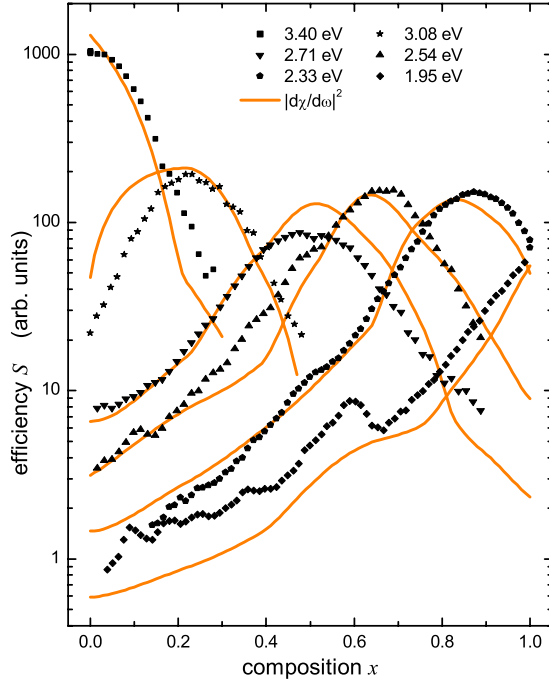


FIG. 2. (Color online) Raman scattering efficiency of SiGe alloys vs the alloy composition for different excitation energies. The symbols refer to the experimental data. From the literature (Ref. 18), the absolute value of S in silicon at 1.9 eV is 1.68×10^{-5} (m Sr) $^{-1}$. The solid lines show the expected resonance curves through the rescaled plot of $|\partial\chi/\partial\omega|^2$, as predicted by the model described in Sec. III C. All the solid lines are rescaled with the same factor.

of the procedure was obtained also from the measurement of the thick samples with constant composition of $x = 0.00, 0.20, 0.40, 0.60, 0.80, 1.00$. A reliability test of our experiment can be obtained by comparing our data with some of the existing data in the literature. Considering the case of pure Si, in Fig. 3 we plot the results of the present work and those of Renucci *et al.*⁴ In order to get a direct comparison we adopted the same corrections for the scattering efficiency S , neglecting the effect of the reflections, which are properly considered in Eq. (3).

B. Raman efficiencies in SiGe alloys

A careful inspection of Fig. 2 reveals that there is a strong modulation of the SiGe Raman efficiency for a fixed excita-

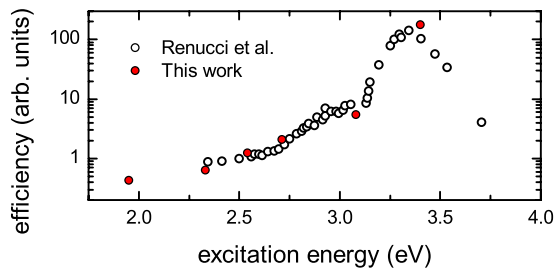


FIG. 3. (Color online) Comparison of our data (filled dots) with the efficiency of Si reported in Renucci *et al.* (Ref. 4) (white dots).

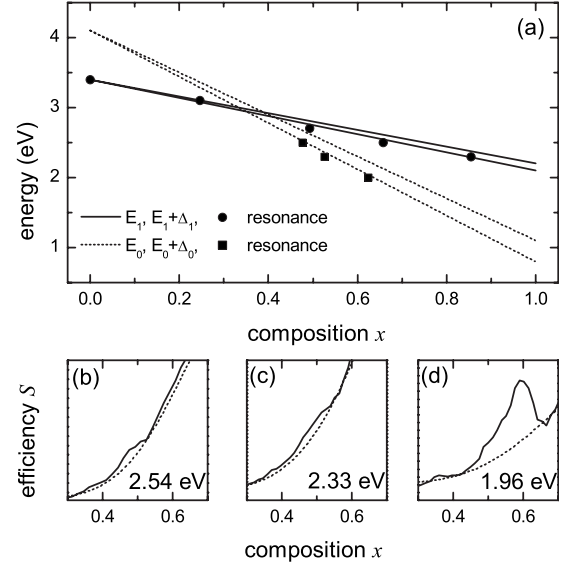


FIG. 4. Panel (a): occurrence of Raman resonance peaks, plotted as energy of excitation light versus composition values corresponding to the resonance maxima. The data are compared to the behavior of the direct electronic transitions in the alloy (from Ref. 21). Panels (b)–(d): details of Fig. 2 showing the small resonances due to the $E_0/E_0+\Delta_0$ transitions. The plots correspond to energies of 1.96 eV, 2.33 eV, and 2.54 eV, respectively. In contrast to Fig. 2, here the scale is linear. The dotted line is a guideline for the eye in order to evidence the contribution of the $E_1/E_1+\Delta_1$ transitions.

tion energy, up to almost 2 orders of magnitude throughout the overall alloy composition range, while, for a fixed composition, the efficiency varies of up to 3 orders of magnitude vs the excitation energy. Another important piece of information is the factor of about 10 between the resonance amplitudes of Si and Ge. Moreover, the lowest resonance enhancement is found for Si_{0.5}Ge_{0.5}. This minimum might be due to the alloy broadening of the $E_1/E_1+\Delta_1$ transitions. The half-width at half maximum of the resonance bands is between $x=0.10$ and $x=0.15$.

By plotting the values of the excitation energies vs the composition values corresponding to the determined resonance peaks [Fig. 4, panel (a)], one can observe a good agreement with the variation of the direct electronic transitions E_1 and $E_1+\Delta_1$ in SiGe as a function of the alloy composition, as reported in Refs. 2–4. In Fig. 4, panels (b)–(d) report in linear scale expanded details of Fig. 2, in order to show that, for some excitation energies, it is possible to clearly observe weak resonances even for the $E_0/E_0+\Delta_0$ transitions, in form of more or less pronounced shoulders of the stronger resonances.

Finally, the fair superposition of the resonances with the bulk transition values (Fig. 4) suggests that in our experiment the strain effect is negligible. This result was expected since it is known from the literature^{22,23} that the effect of a 0.3% strain is to shift the $E_1/E_1+\Delta_1$ and $E_0/E_0+\Delta_0$ transitions of a very small amount below 100 millielectron volts.

So far, we considered the intensity I_{SiGe} as the sum of the three main bands of SiGe, and therefore the efficiency S_{SiGe} was related to the whole scattered radiation. In this section we analyze the behavior of the three single bands and we

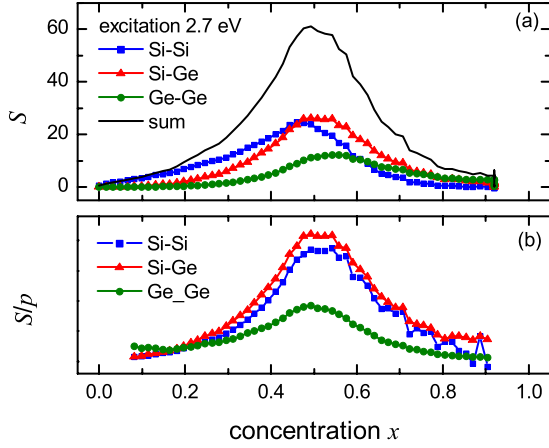


FIG. 5. (Color online) Panel (a): contribution to the total scattering efficiency S from the three bands related to Si-Si, Si-Ge, and Ge-Ge vibrations. The values of S are normalized to the scattering efficiency of CaF_2 . Panel (b): the same data of panel (a) normalized with respect to the probability p of finding in the alloy Si-Si, Si-Ge, or Ge-Ge bonds.

extract the values of their contribution to the total efficiency S . The situation for the excitation at 2.7 eV is shown in Fig. 5, where we observe that the relative contribution of each of the three bands to the total S changes with the composition x . Moreover, the resonance of the three bands occurs at three different values of x . Of course, this is caused by the fact that the intensity of the three single bands depends also on the probability p of finding in the alloy Si-Si, Si-Ge, or Ge-Ge bonds. The probability is a function of the composition as $(1-x)^2$, $x(1-x)$, and x^2 , respectively. In Fig. 5, panel (b), we show the same results of panel (a) after the normalization over the probability p . In this case, as expected, all the three curves show a maximum for the same composition.

C. Physical origin of the resonance

In this section we compare our experimental results with the theoretical framework about resonance phenomena in diamond-type semiconductors developed by Cardona.²⁴ It is possible to check the validity of the extension of the previous works for all the compositions by recalling that the Raman efficiency is proportional to the factor $|\delta\chi|^2$, which is the square modulus of the electrical susceptibility variation induced by the phonon, described by the normal coordinate ξ . For silicon and germanium, if one takes into account the $E_1/E_1 + \Delta_1$ transitions only, the quantity $\delta\chi$ is proportional to the following combination of optical functions:

$$\delta\chi \propto \frac{\sqrt{2}}{\sqrt{3}} d_{3,0}^5 \left[\frac{2(\chi^+ - \chi^-)}{\Delta_1} \right] + \frac{d_{1,0}^5}{2\sqrt{3}} \frac{d\chi}{d\omega}, \quad (4)$$

where χ^+ and χ^- are the contributions to the electric susceptibility due to the two split-off bands. The symbols d are deformation potentials and Δ_1 is the split-off energy. In the literature, the only data available for χ^+ and χ^- were measured for pure Ge by photoreflectance²⁵ but it is possible to make some approximations to roughly compare our data to the model proposed for pure Si and Ge. The approximation consists in assuming that $\chi^+(\omega) \approx \chi^-(\omega - 2\pi\Delta_1/h)$. Another consideration is that for small values of x the energy Δ_1 is much smaller than the bandwidth of the efficiency resonance.^{4,25} Within this assumption, the expression in square brackets of Eq. (4) tends to the derivative of χ . Therefore we can approximate Eq. (4) with the following expression:

$$\delta\chi \propto \left(\frac{\sqrt{2}}{\sqrt{3}} d_{3,0}^5 + \frac{d_{1,0}^5}{2\sqrt{3}} \right) \frac{d\chi}{d\omega}. \quad (5)$$

The derivative of χ is a quantity that can be readily found since the optical function of SiGe alloys are reported in detail for the whole range of compositions.¹⁹ In Fig. 2 we superimposed the values of $|d\chi/d\omega|^2$, adequately rescaled (all with the same factor) in order to compare them with the experimental data. There is indeed a good agreement both in the occurrence of the resonance and in the relative amplitudes. The mismatch is within a factor of about 2, which can be considered reasonable taking into account both the uncertainties affecting the experimental data and the crude approximation of Eq. (5). In fact, the approximation of Eq. (5), in principle, is not valid for Ge-rich alloys, where Δ_1 increases to up to 0.3 eV, a value that is comparable to the width of the resonance.

D. Conclusions

The Raman scattering efficiency in SiGe alloys was measured for the whole range of alloy composition and for several excitation energies. The scattering efficiency showed a strong variation of up to 3 orders of magnitude throughout the overall compositional range. The spectral features of the resonance curves were attributed to the electronic transitions in the solid and explained in terms of variation in the susceptibility. The role of the three bands to the overall scattering efficiency was evidenced and discussed. Our results were compared with the existing literature.

ACKNOWLEDGMENTS

The authors are grateful to M. Milani and F. Pezzoli for useful discussions. They also acknowledge the technical support of E. Cinquanta and E. Boria. This work was supported by CARIPLO Foundation through the MANDIS project.

- ¹J. B. Renucci, M. A. Renucci, and M. Cardona, *Solid State Commun.* **9**, 1235 (1971).
- ²F. Cerdeira, W. Dreybrodt, and M. Cardona, *Solid State Commun.* **10**, 591 (1972).
- ³A. Pinczuk and E. Burstein, *Surf. Sci.* **37**, 153 (1973).
- ⁴J. Renucci, R. N. Tyte, and M. Cardona, *Phys. Rev. B* **11**, 3885 (1975).
- ⁵F. Cerdeira, M. I. Alonso, D. Niles, M. Garriga, M. Cardona, E. Kasper, and H. Kibbel, *Phys. Rev. B* **40**, 1361 (1989).
- ⁶F. Cerdeira, A. Pinczuk, and J. C. Bean, *Phys. Rev. B* **31**, 1202 (1985).
- ⁷F. Cerdeira, A. Pinczuk, J. C. Bean, B. Batlogg, and B. A. Wilson, *J. Vac. Sci. Technol. B* **3**, 600 (1985).
- ⁸D. Bougeard, P. H. Tan, M. Sabathil, P. Vogl, G. Abstreiter, and K. Brunner, *Physica E* **21**, 312 (2004).
- ⁹A. G. Milekhin, A. I. Nikiforov, M. Yu, O. P. Pchelyakov, S. Schulze, and D. Zahn, *Phys. Solid State* **46**, 92 (2004).
- ¹⁰A. B. Talochkin and V. A. Markov, *Nanotechnology* **19**, 275402 (2008).
- ¹¹F. Pezzoli, E. Bonera, E. Grilli, M. Guzzi, S. Sanguinetti, D. Chrastina, G. Isella, H. von Känel, E. Wintersberger, J. Stangl, and G. Bauer, *Mater. Sci. Semicond. Process.* **11**, 279 (2008).
- ¹²E. Bonera, F. Pezzoli, A. Picco, G. Vastola, M. Stoffel, E. Grilli, M. Guzzi, A. Rastelli, O. G. Schmidt, and L. Miglio, *Phys. Rev. B* **79**, 075321 (2009).
- ¹³G. Isella, D. Chrastina, B. Rössner, T. Hackbarth, H. J. Herzog, U. König, and H. von Känel, *Solid-State Electron.* **48**, 1317 (2004).
- ¹⁴T. C. Damen, S. P. S. Porto, and B. Tell, *Phys. Rev.* **142**, 570 (1966).
- ¹⁵F. Pezzoli, L. Martinelli, E. Grilli, M. Guzzi, S. Sanguinetti, M. Bollani, D. Chrastina, G. Isella, H. von Känel, E. Wintersberger, J. Stangl, and G. Bauer, *Mater. Sci. Eng., B* **137**, 315 (2007).
- ¹⁶M. Cardona and G. Guntherodt, *Light Scattering in Solids*, Topics in Applied Physics Vol. I, 2nd ed. (Springer-Verlag, Berlin, 1975).
- ¹⁷G. A. Slack and S. F. Bartram, *J. Appl. Phys.* **46**, 89 (1975).
- ¹⁸M. Cardona and G. Guntherodt, *Light Scattering in Solids*, Topics in Applied Physics Vol. II, 2nd ed. (Springer-Verlag, Berlin, 1982).
- ¹⁹J. Humlíček, M. Garriga, M. I. Alonso, and M. Cardona, *J. Appl. Phys.* **65**, 2827 (1989).
- ²⁰E. D. Palik, *Handbook of Optical Constants of Solids* (Elsevier, New York, 1998).
- ²¹C. Penn, T. Fromherz, and G. Bauer, *Properties of SiGe and SiGe:Carbon* (INSPEC, London, 1999).
- ²²T. Ebner, K. Thonke, R. Sauer, F. Schäffler, and H. J. Herzog, *Phys. Rev. B* **57**, 15448 (1998).
- ²³H. Lee, *Thin Solid Films* **313-314**, 167 (1998).
- ²⁴M. Cardona and G. Guntherodt, *Light Scattering in Solids*, Topics in Applied Physics, 2nd ed. (Springer-Verlag, Berlin, 1982).
- ²⁵D. D. Sell and E. O. Kane, *Phys. Rev.* **185**, 1103 (1969).